© 2021 IEEE. Personal use of this material is permitted. Permission from IEEE must be obtained for all other uses, in any current or future media, including reprinting/republishing this material for advertising or promotional purposes, creating new collective works, for resale or redistribution to servers or lists, or reuse of any copyrighted component of this work in other works.2021 Joint IEEE International Symposium on Electromagnetic Compatibility, Signal and Power Integrity, EMC Europe

Analysis and Estimation of Electromagnetic Energy Coupled into IC packages

Hui Tang
School of Information Science and Technology, Nantong University
Nantong, China
huitang16@hotmail.com

Arunkumar H. Venkateshaiah
Department of Electronic Engineering
University of York
York, UK
arunkumar.venkateshaiah@york.ac.uk

John F. Dawson
Department of Electronic Engineering
University of York
York, UK
john.dawson@york.ac.uk

Andrew C. Marvin
Department of Electronic Engineering
University of York
York, UK
andy.marvin@york.ac.uk

Martin P. Robinson
Department of Electronic Engineering
University of York
York, UK
martin.robinson@york.ac.uk

Jie Ge
School of Electronic Information Engineering, Nantong Vocational University,Nantong, China
eastriver@qq.com

***Abstract*—Interference analysis and prediction in integrated circuits (ICs) is of significant interest to the Electromagnetic Compatibility (EMC) community. In this paper, an easy method is introduced to estimate the level of RF interference coupled into ICs through the package. Although IC packages are in different forms with large number of pins, the presented analysis method provides a general solution and greatly shortens the computation time by creating a simplified model with consideration of the cross coupling between pins. The expected voltage range at the outer ends and inner ends of the pins are also investigated for resistive loads. The levels of energy coupled into PCB traces and packages are also compared for immunity analysis.**

Index Terms—*Cross coupling, Absorbed power, IC package, Electromagnetic Interference*

I. INTRODUCTION

The development of high-performance electronic systems continuously requires increasing integration levels. More and more integrated circuits (ICs) have been applied in modern products and applications, which implies that the absorption of electromagnetic power through IC package affects the immunity of inner circuits and then influences the overall performance of the system. There have been lots of efforts and standards for modeling, analyzing and measuring electromagnetic immunity (EMI) and emission (EMS) of ICs [1]-[7].

However the calculation of the power coupled into IC packages for the Electromagnetic Compatibility (EMC) are time consuming and storage intensive. The complexity of the package types and large number of pins hamper the research progress. Highly integrated circuits and compact size bring cross coupling between pins. From the package perspective, the cross coupling is so complicated that suitable equivalent circuits for calculation are not easy to obtain.

The effect of contents on the shielding effectiveness (SE) of enclosures has been considered in [8]-[13], where it can be seen that the energy absorbed into printed circuit boards, and other components tends to increase the SE. We also measured average absorption cross-section (AACS) of printed circuit boards (PCBs) [9], [13], [14] to establish the extent of the previous effect. However, it is also of interest to establish how energy absorbed by a PCB is absorbed into the ICs on board. In this paper, based on our previous work, we investigate the electromagnetic power coupled into ICs through the package. All of the results in this paper are computed using a full-wave Finite Integration Technique solver [15]. An easy prediction method is proposed for rapid estimation of the level of electromagnetic interference coupled and absorbed at the inner loads of IC pins. According to the analysis results, the complicated package categories and huge pin numbers are ignored. Instead, a simplified model is proposed and used to compute the absorbed power quickly, starting from an example of an IC Package of the Leaded Quad Flatpack type with 52 pins (LQFP 52). The impact of the loads on the absorption of the power is also investigated. We chose to ignore losses in this study for the sake of simplicity and as we have seen in other work, not yet published, that their effect on

The research leading to these results has received funding from the European Union's Horizon 2020 research and innovation programme under the Marie Skłodowska-Curie grant agreement No 812.790 (MSCA-ETN PETER). This publication reflects only the author's view, exempting the European Union from any liability. Project website: http://etn-peter.eu/. The work of H Tang and J Ge was also supported by Jiangsu-UK 20+20 World Class University Consortium and the Basic Science Research Program of Nantong under Grant JC2019001 and JC2019113.

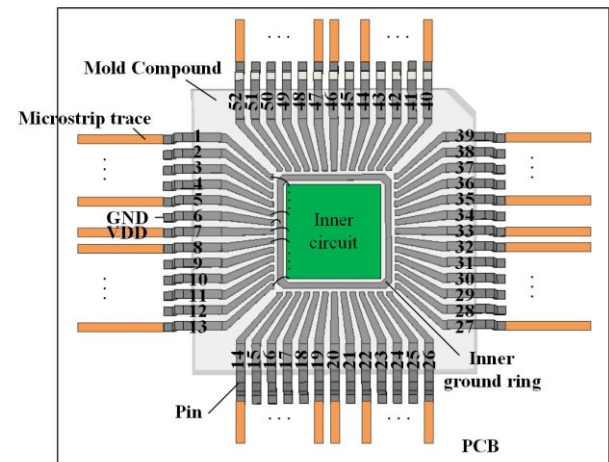

(a)

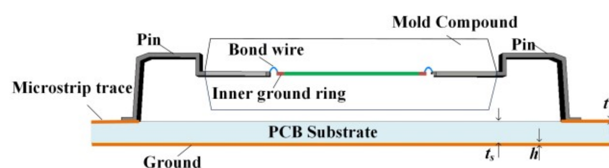

(b)

Fig. 1. Layout of the traces of the IC package in our design. (a) Top view and (b) side view.

energy absorbed is small. The study is conducted with using an ensemble of plane waves evenly distributed in angle of arrival and polarisation representative of a reverberant environment, at frequencies up to 10 GHz.

In Section II, the influence of grounding condition, the cross coupling among IC pins are analysed and a simplified model to estimate the absorbed electromagnetic energy is formed. The power absorbed at the loads are presented and compared in Section III. In Section IV the energy absorbed by the package is compared with that absorbed by a PCB track. Finally, the conclusions are reached.

II. Package Model and Analysis

As shown in Fig. 1, a 52-pin LQFP package is mounted on a printed circuit board (PCB) with microstrip traces connected to the pins and PEC wires linking the inner ends of the leadframe to the IC bond pads. The external electromagnetic plane wave with electric field $\vec{E}$ and wave vector $\vec{k}$ is shown in Fig. 2. Here θ and φ are the polar angle and azimuth angle of the incidence, respectively. γ is the polarisation angle of the incident field. The external wave excites electric currents on both the microstrip traces and the pins which flow into the IC and then power is absorbed by a load placed between the bond-pad and the local ground ring.

The absorption of electromagnetic power in microstrip traces has been described previously by Xie et al [16]. To match this previous work, we use a FR4 substrate with a dielectric constant $\varepsilon_r = 4.4$, a thickness $t_s = 1.55$ mm and a size of 40 mm × 40 mm as the test PCB. The characteristic impedance of the microstrip traces are set as $Z_C = 115\ \Omega$ with a thickness of $t = 18$ µm and a width of $w = 0.45$ mm to match the pins of the IC package.

The absorbed power at the inner ends of the pins is the focus of this paper. Different from the PCB traces on which the RF signals propagate, some power and ground (PG) traces that connect to the IC package are necessary and all the pins are very close to each other. The number and location of the PG pins have a big impact on signal transmission into the IC. The largest distance between two adjacent pins is 0.25 mm on a LQFP 52 package, which is narrow enough to cause significant cross coupling between the pins. In order to find a simplified model to estimate electromagnetic energy coupled into the package, the influence of the PG traces and cross coupling between pins are studied in this section.

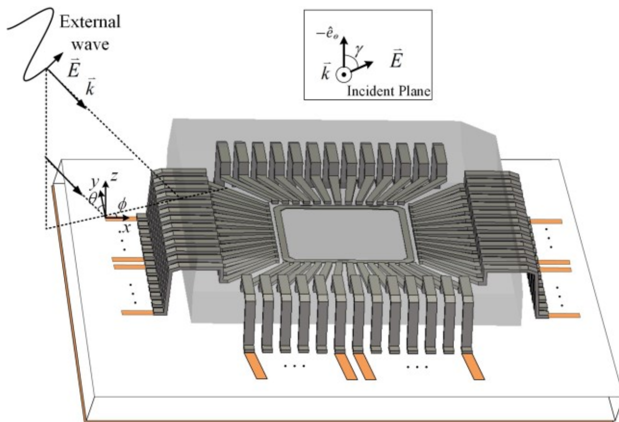

Fig. 2. Power coupled into an IC package.

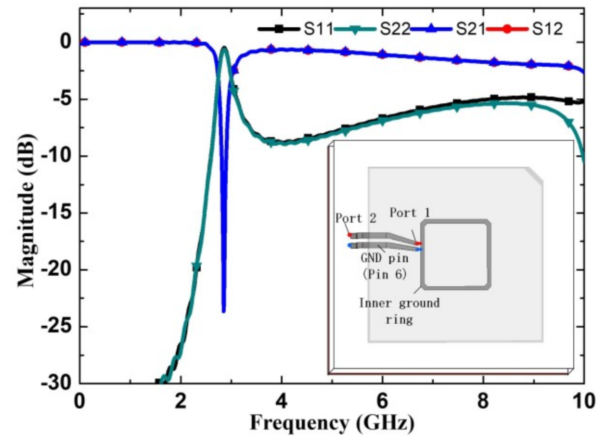

(a)

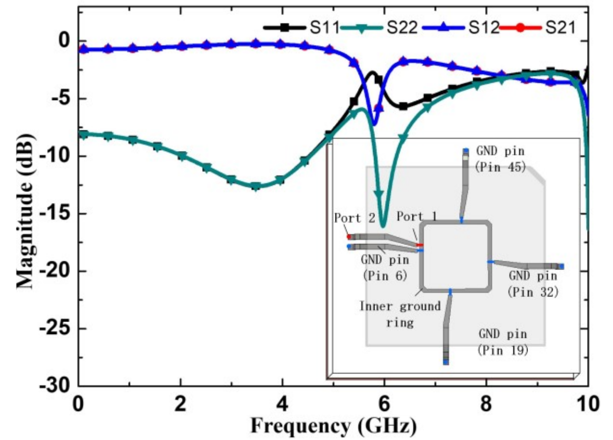

(b)

Fig. 3. Different models for Pin 5 (terminated by 115 Ω outer port and 50Ω inner port). (a) S-parameters of one-side grounding model. (b) S-parameters of four-side grounding model.

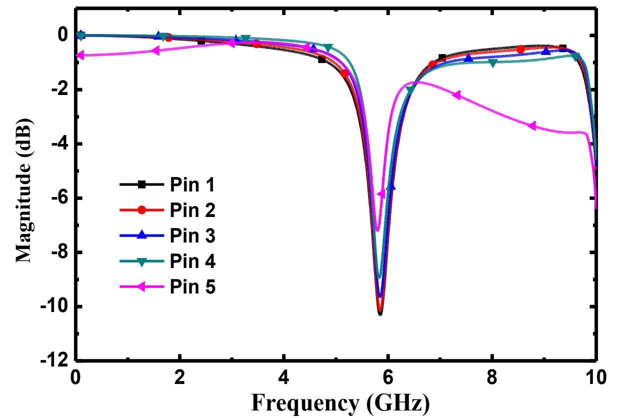

Fig. 4. |S12| of different signal pins with four-side GND pins.

A. *Influence of PG traces*

Here Pin 5, as shown in Fig. 1, is taken for example firstly, the conclusion also applies to other pins as shown later. Based on our design, one- and four-side grounding models are built for Pin 5 to study the influence of the number of the GND pins, as shown in Fig. 3 (a) and (b). In the models, GND pins are connected to an inner ground ring and the PCB ground plane. The object pin is regarded as a dual-port network with 115 Ω outer port and 50 Ω inner port, to match the 115 Ω characteristic impedance microstrip traces and the input

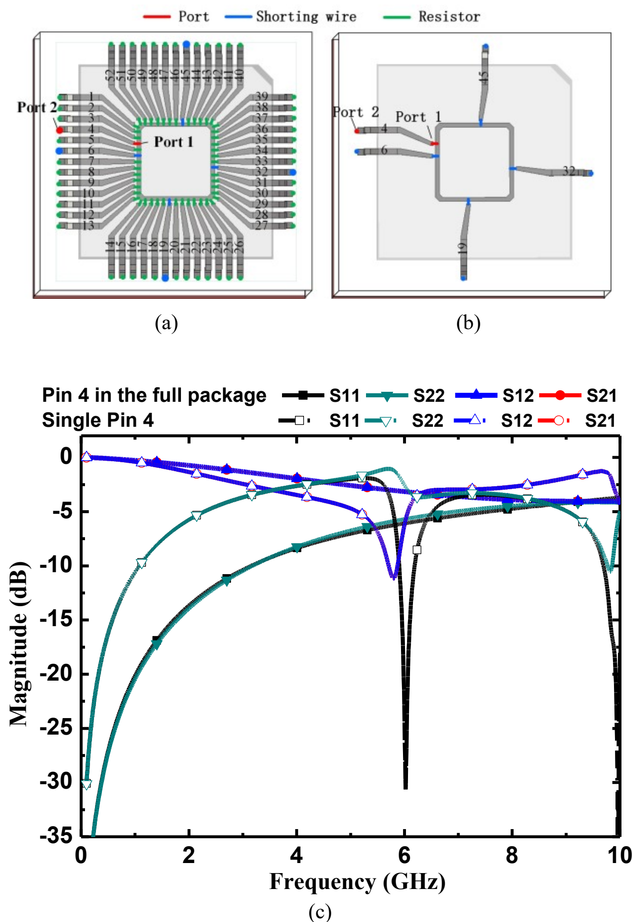

Fig. 5. Pin 4 terminated by ports in different models and its S-parameters. (a) Full package model. (b) Single signal pin model. (c)

impedance of conventional microwave circuits respectively. The S-parameters of Pin 5 for different grounding models are depicted in Fig. 3, too. It is seen that there is a stopband at 2.85 GHz in the one-side model and one at 5.83 GHz in the four-side model, which come from the resonance of the inner ground ring. Good grounding increases the resonant frequency. These results imply that more GND pins provide a wider transmission band for signals.

As for the impact of the location of signal pins, we use the models with different signal pins to study. Fig. 4 presents |S21| of different pins with four-side GND pins. It shows a very slight changes of the |S21| of the different pins and indicates that the position of the signal pin is not critical for the transmission ability in this case. In other words, good grounding condition is necessary for all pins to transmit signals properly.

B. Influence of cross coupling between pins

Pin 4 is studied in models with different numbers of adjacent pins to investigate the influence of cross coupling between pins. Studies show that the effect on other pins are similar to that on Pin 4, however, owing to space constraints, only the latter is considered in this paper. Fig. 5 (a) shows that Pin 4 is still terminated by 115 Ω outer port and 50 Ω inner port in the full IC package model, in which all other signal pins are included and loaded by 115 Ω outer resistors and 50 Ω inner resistors. Fig. 5 (b) presents single Pin 4 model in which other signal pins are deleted. The s-parameters of Pin 4 in the two models are shown in Fig. 5 (c). The comparison indicates the |S21| and |S12| curves in the full package model are more

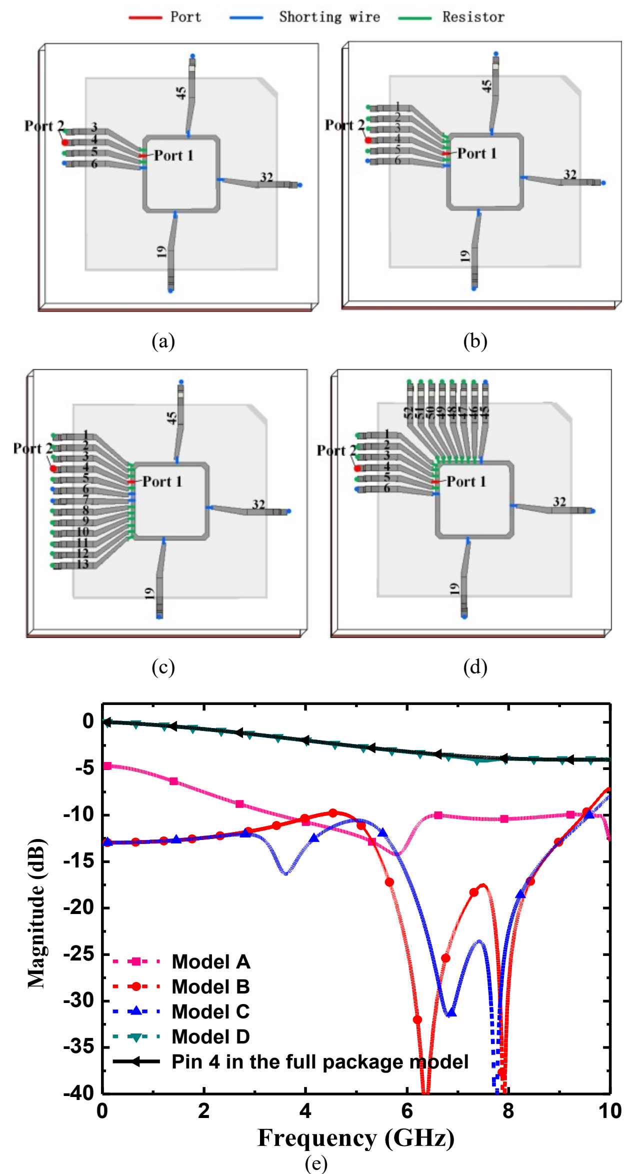

Fig. 6. Pin 4 terminated by ports in different models and its S-parameters. (a) Model A, (b) Model B, (c) Model C, (d) Model D, and (e) comparison of |S21| in different models.

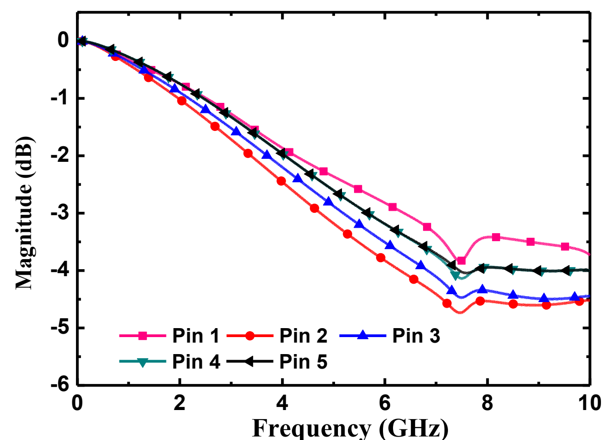

Fig. 7. |S21| of different pins in the simplified model of Fig.6 (d).

flat with less insertion loss and without an obvious stopband, because the cross coupling between pins helps cancel out the

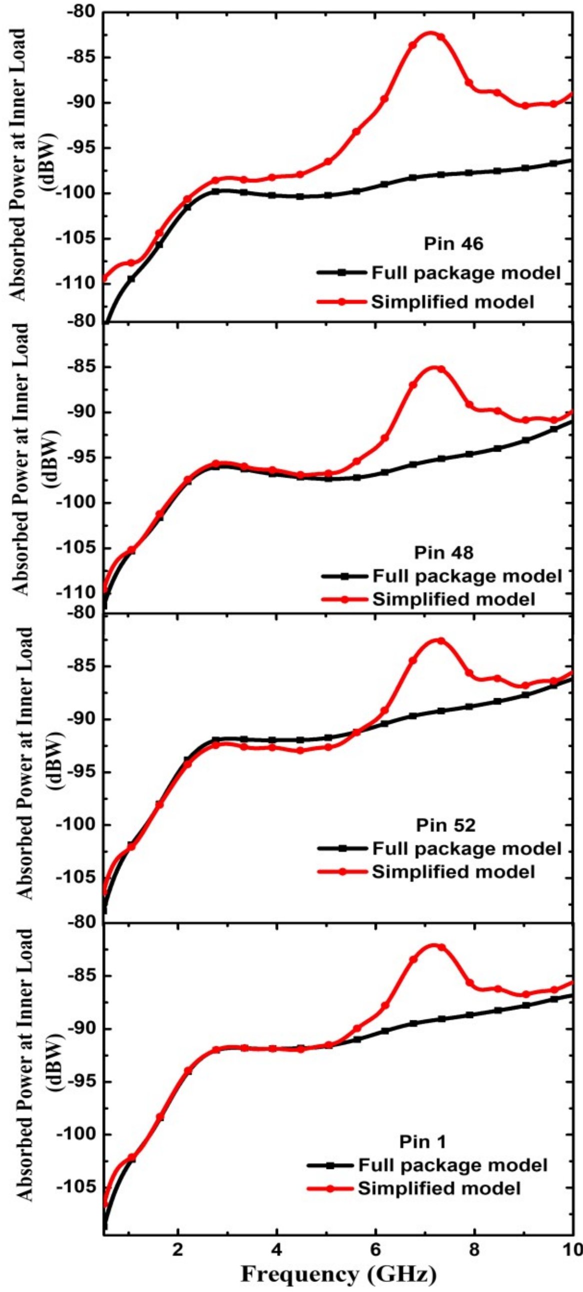

Fig. 8. Comparison of absorbed power at the inner loads in the full package model and the simplified model of Fig.6 (d).

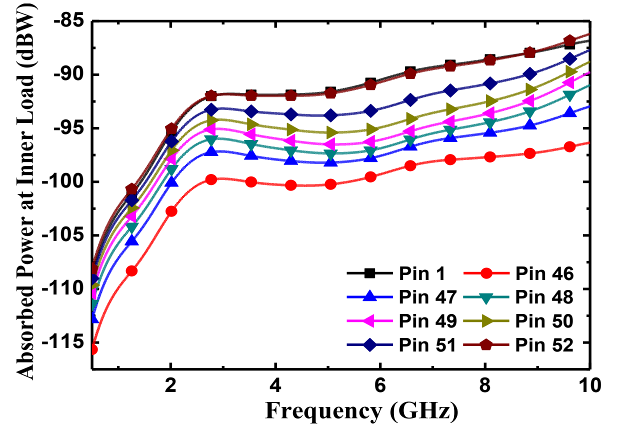

Fig. 9. Comparison of absorbed power at different inner loads in the full package model.

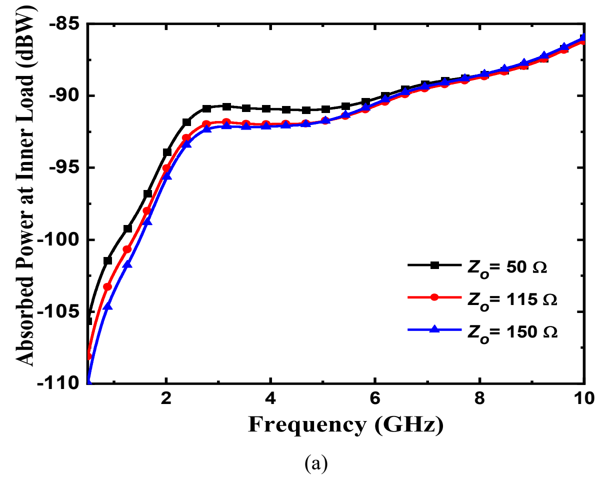

(a)

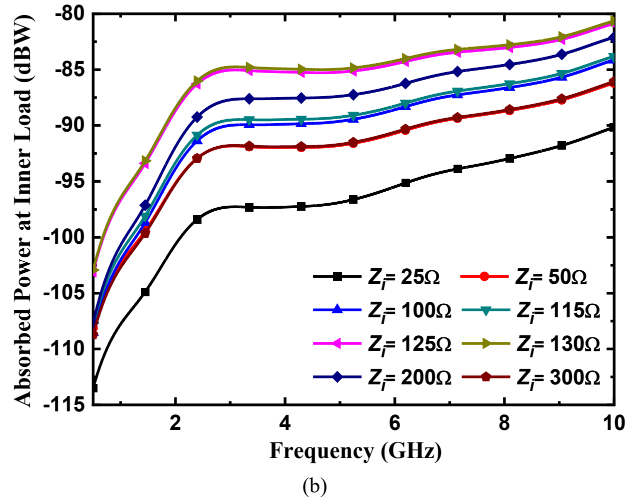

(b)

Fig. 10. Power absorbed through Pin 1 affected by (a) the load at the outer end with a 50 Ω inner resistance, and (b) the load at the inner end with a

stopband and improve the transmission ability of the target pin with resistive terminations.

In order to find out the influential pins to Pin 4, models including different numbers of adjacent pins are built and studied, as shown in Fig. 6 (a)-(d). The |S21| parameters of Pin 4 in different models are compared in Fig. 6 (e). It can be seen that the signal pins cannot be analyzed separately. Only in Model (d), the transmission gain |S21| of Pin 4 is very close to that in the full package model. Thus, the smallest unit for Pin 4 to analyse contains at least 13 pins surrounded by two adjacent GND pins, which is almost a quarter of the full package.

To verify that the model shown in Fig 6 (d) applies to other pins and is suitable for simplification, the transmission gains |S21| of different pins in the simplified model are investigated as shown in Fig. 7. It is obvious that there are very slight differences between them. Pins in Model (d) have the similar transmission ability as they do in the full package model. And because of the symmetry of the structure, a universal simplified model for each pin of the LQFP 52 except GND ones has been achieved.

III. Power Absorbed at Inner Resistors

The simplified Model (d) is used in determining the EMC of the IC package in this section. The absorption of

electromagnetic energy in IC packages affects the overall immunity and the emissions of equipment, so the absorbed power into the packages is important to study. The power absorbed at the inner resistors of the pins is calculated both in the full package model and the proposed simplified model. Here, all the signal pins are terminated by 115 Ω outer resistors and 50 Ω inner resistors, with four-side GND pins. The average power absorbed by the loads [16] is written as

$$\left\langle P_{o,i} \right\rangle = \left\langle \left| V_{o,i} \right|^2 \right\rangle \mathrm{Re}\left(\frac{1}{Z_{o,i}^{\ *}} \right) \tag{1}$$

where V_o and V_i are the voltages at the outer and inner ends with the terminal loads Z_o and Z_i, respectively. The mean square magnitude of the voltage at the end of the pin excited by stochastic electromagnetic fields inside a reverberation chamber is given by

$$\left\langle \left| V_{o,i} \right|^2 \right\rangle = \frac{1}{2\pi} \int_0^{2\pi} \frac{1}{2} \int_0^{\pi/2} \frac{1}{\pi} \int_0^{\pi} \frac{1}{2\pi} \int_0^{2\pi} \left| V_{o,i} \right|^2 \sin\theta d\alpha d\gamma d\theta d\phi \tag{2}$$

where $\langle \ \rangle$ denotes the average over all the incident angles θ and φ, the polarisation angle γ, and the phase angle α. The polar angle $\theta \in [0, \pi/2]$, because we only consider the plane wave from upper hemisphere couples to the package. In this paper, the absorbed power in the inner ends of the pins are discussed, thus the power is calculated using V_i.

The models are illuminated with 64 individual plane waves chosen based on the Gauss-Legendre Quadrature method [8], [17] and our previous work [18] to achieve optimum results with the minimum number of simulations.

Table 1 Comparison of the calculation time and occupied memory

Model	Calculation time	Peak memory used	Result file size
Full package	5 h 7 m 59 s	383652 kB	3520 MB
Simplification	2 h 5 m 16 s	176936 kB	932 MB

*CPU: Intel Core i7-8th Gen @2.20GHz
*RAM: 64.0GB
*Number of CPU threads: 6

It takes less time and less computer memory to calculate the simplified model than the full package model. The comparison of the calculation time and occupied memory is shown in Table 1. As shown in Fig. 8, the curves of the simulated absorbed power at the inner loads of the pins in the simplified model and in the full package model are close to each other in the frequency range lower than 6 GHz. While in the frequency range near 7 GHz, the powers in the simple model are higher than those in the full package model. The farther the pin from the GND pin, the smaller the difference between the two results. The largest difference of the absorbed power at Pin 52 between in the simplified model and in the full model is about 6 dB. Almost the same value happens at Pin 1. It is acceptable when predicting the power. According to the simulated results of the full package model shown in Fig.9, as the pin gets far away from the GND pins, the simulated absorbed power at its inner load increases. In order to include more pins, we study Pin 46-52 as well as Pin 1. The curves of two pins, Pin 1 and Pin 52 which are far away from the GND pins, are almost the same. The power coupling through Pin 1 or Pin 52 is the highest in the package. From the point of EMC, the largest absorbed power should be considered to estimate the interference coupled into ICs, which can be quickly calculated using the proposed simplified model.

The influences of the loads at the outer and inner ends of the target pin on the power absorbed at the inner load are also studied here. Fig. 10 (a) depicts the power at the inner load Z_i = 50 Ω of Pin 1 with the according load Z_o at the trace end (the outer end of the pin) varying from 50 Ω to 150 Ω. The smaller the resistance Z_o at the trace end, the larger the absorbed power at Z_i. It is seen that the power shows a change of 1.18 dB at 4 GHz and remains almost unchanged at frequencies higher than 6 GHz. Fig. 10 (b) shows the power curves for different inner loads Z_i with Z_o = 115 Ω at the outer end. It is seen that the inner load Z_i has a big impact on the absorbed power. It can be seen that maximum power is absorbed when the inner load is about 130 Ω. The difference between the power absorbed at the 25 Ω and 130 Ω inner resistances over the frequency range of 0.5-10 GHz reaches 10.74 dB.

IV. Comparison of Track and Package Coupling

In [16], the energy coupled into PCB traces is considered, and here we compare the levels of PCB trace and track coupling, in order to determine whether package coupling should be taken into account when we wish to determine the total energy coupled into a circuit for immunity analysis.

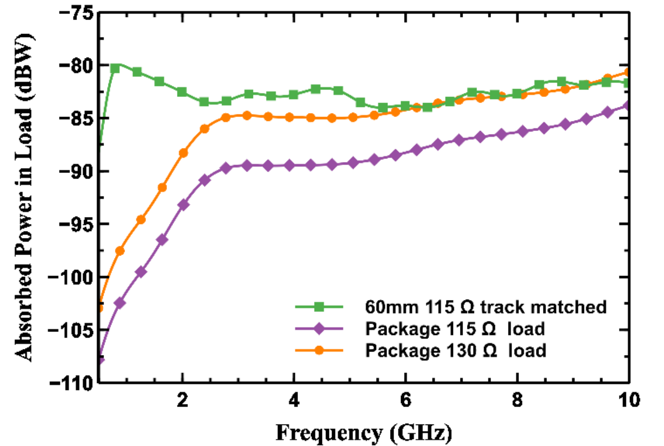

Fig. 11. Comparing the power absorbed by a 1.55mm high, 60mm long, 115 ohm microstrip track with that absorbed by 115 Ω and 130 Ω loads on the package pin 1 inner terminal.

Fig. 11 compares the power absorbed into the inner terminal of the IC package alone, with the power absorbed by a matched load on a 115 stripline trace 1.55mm in height on FR4 material, based on Fig.6 in [16]. It can be seen that the power absorbed by the package, at frequencies above 2 GHz, is comparable to that of a 60 mm long track if matched with the resistive load that dissipates maximum power. The track, being physically larger reaches its highest level of power at a lower frequency than the package.

V. Conclusions and Further Work

The transmission features of a 52-pin LQFP has been analysed to obtain a simplified method to estimate the level of RF interference coupled into ICs through the package initially with resistive loads. To include the cross coupling into the simplified model, S-parameters of different models have been studied. The coupled electromagnetic powers into the simplified model and the full package model have been

compared. In our investigated frequency range up to 10 GHz, the calculated absorbed power of the pins which are farthest away from the GND pins in the simplified model is suitable to estimate electromagnetic energy coupled into the IC package. The process is time-saving and also saves the computer memory. The inner load at the output of the IC package has a big impact on the absorbed power.

This work will benefit from further validation by measurement and a RF detector IC is currently being designed so that we can directly deduce the pickup on the IC bond pad. Also this will allow us to see the effect of real circuit loads rather than the resistive terminations used here.

As we have only considered the package, and a single track here, there is also further work to do looking at the interaction between multiple track on the level of energy absorbed, and determining the combined levels when track and package are considered together.

In this preliminary work we have not yet been able to consider the realistic range of termination impedances for the inner pads. These data will be derived and incorporated into the model when the RF detector IC becomes available.

REFERENCES

[1] *IEC 62132-4:2006, Integrated circuits - Measurement of electromagnetic immunity 150 kHz to 1 GHz - Part 4: Direct RF power injection method*, 2006.

[2] E.-P. Li, X.-C. Wei, A. C. Cangellaris, E.-X. Liu, Y.-J. Zhang, M. D'Amore, J. K., and T. Sudo, "Progress review of electromagnetic compatibility analysis technologies for packages, printed circuit boards, and novel interconnects," *Electromagnetic Compatibility, IEEE Transactions on*, vol. 52, no. 2, pp. 248-264, May 2010.

[3] J. Kim and H. H. Park, "A novel IC-stripline design for near-field shielding measurement of on-board metallic cans," *Electromagnetic Compatibility, IEEE Transactions on*, vol. 59, no. 2, pp. 710-716, APR. 2017.

[4] Alaeldine, R. Perdriau, M. Ramdani, J.-L. Levant, M. Drissi, "A direct power injection model for immunity prediction in integrated circuits," *Electromagnetic Compatibility, IEEE Transactions on,* vol. 50, no. 1, pp. 52-62, Feb. 2008.

[5] H.-H. Chuang, C.-J. Hsu, J. Hong, C.-H. Yu, A. Cheng, J. Ku, and T.-L. Wu, "A broadband chip-level power-bus model feasible for power integrity chip-package codesign in high-speed memory circuits," *Electromagnetic Compatibility, IEEE Transactions on*, vol. 52, no. 1, pp. 235-239, Feb. 2010.

[6] S. O. Land, M. Ramdani, and R. Perdriau, "Dominant coupling mechanism for integrated circuit immunity of SOIC packages up to 10 GHz," *Electromagnetic Compatibility, IEEE Transactions on*, vol. 60, no. 4, pp. 965-970, Aug. 2018.

[7] M. G. Novellas, R. Serra, M. Rose, and R. Secareanu "Efficient modeling of multistage integrated circuit passive isolation structures," *Electromagnetic Compatibility, IEEE Transactions on*, vol. 60, no. 2, pp. 544-547, Apr. 2018.

[8] I.D. Flintoft, S.J. Bale, A.C. Marvin, M. Ye, J.F. Dawson, M.Z. Changyong Wan, S.L. Parker, and M.P. Robinson, "Representative contents design for shielding enclosure qualification from 2 to 20 GHz," *Electromagnetic Compatibility, IEEE Transactions on*, vol. 60, no. 1, pp. 173–181, Feb. 2018.

[9] I.D. Flintoft, S.L. Parker, S.J. Bale, A.C. Marvin, J.F. Dawson, and M.P. Robinson, "Measured average absorption cross-sections of printed circuit boards from 2 to 20 GHz," *Electromagnetic Compatibility, IEEE Transactions on*, vol. 58, no. 2, pp. 553–560, Apr. 2016.

[10] A.C. Marvin, J.F. Dawson, S. Ward, L. Dawson, J. Clegg, and A. Weissenfeld, "A proposed new definition and measurement of the shielding effect of equipment enclosures," *IEEE Transactions on Electromagnetic Compatibility*, vol. 46, no. 3, pp. 459–468, 2004.

[11] J.F. Dawson, A.C. Marvin, M. Robinson, and I.D. Flintoft, "On the meaning of enclosure shielding effectiveness," *2018 International Symposium on Electromagnetic Compatibility - EMC EUROPE*, Amsterdam: 2018, pp. 746–751.

[12] D.W.P. Thomas, A. Denton, T. Konefal, T.M. Benson, C. Christopoulos, J.F. Dawson, A.C. Marvin, and J. Porter, "Characterisation of the shielding effectiveness of loaded equipment enclosures," *Electromagnetic Compatibility, 1999. EMC York 99. International Conference and Exhibition on (Conf. Publ. No. 464)*, 1999, pp. 89–94.

[13] S.L. Parker, I.D. Flintoft, A.C. Marvin, J.F. Dawson, S.J. Bale, M.P. Robinson, M. Ye, C. Wan, and M. Zhang, "Predicting shielding effectiveness of populated enclosures using absorption cross section of PCBs," *2016 International Symposium on Electromagnetic Compatibility - EMC EUROPE*, 2016, pp. 324–328.

[14] S. Parker, I. Flintoft, A. Marvin, J. Dawson, S. Bale, M. Robinson, M. Ye, C. Wan, and M. Zhang, "Changes in a printed circuit board's absorption cross section due to proximity to walls in a reverberant environment," *Electromagnetic Compatibility (EMC), 2016 IEEE International Symposium on*, Ottawa, Canada: 2016, pp. 818–823.

[15] "CST Studio Suite. 2019.," [Online]. Available: www.3ds.com/products-services/simulia/products/cst-studio-suite: Dassault Systemes, .

[16] H. Xie, J.F. Dawson, A.C. Marvin, and M.P. Robinson, "Numerical and theoretical analysis of stochastic electromagnetic fields coupling to a printed circuit board trace," *Electromagnetic Compatibility, IEEE Transactions on*, vol. 62, no. 4, pp. 1128-1135, Aug. 2020.

[17] K. Atkinson, "Numerical integration on the sphere," *J. Aust. Math. Soc. B*, vol. 23, pp. 332–347, 1982.

[18] A. H. Venkateshaiah, H. Xie, J. F. Dawson, A. C. Marvin, L. Dawson and M. P. Robinson, "Coupling of energy into PCB traces in a reverberant environment: absorption cross-section and probability of susceptibility," *2020 International Symposium on Electromagnetic Compatibility - EMC EUROPE*, Rome, Italy, 2020, pp.1-6, doi: 10.1109/EMCEUROPE48519.2020.9245804.